STRUCTURAL PERFORMANCE OF A COMPRESSIVELY LOADED FOAM-CORE HAT-STIFFENED TEXTILE COMPOSITE PANEL

Damodar R. Ambur and Benson H. Dexter
NASA Langley Research Center
Hampton, VA 23681-0001

Presented at the AIAA/ASME/ASCE/AHS/ASC 37th Structures,
Structural Dynamics, and Materials Conference
Salt Lake City, Utah
April 15-17, 1996

AIAA Paper No. 96-1368

STRUCTURAL PERFORMANCE OF A COMPRESSIVELY LOADED FOAM-CORE HAT-STIFFENED TEXTILE COMPOSITE PANEL

Damodar R. Ambur* and Benson H. Dexter**
NASA Langley Research Center
Hampton, VA 23681-0001

Abstract

A structurally efficient hat-stiffened panel concept that utilizes a structural foam as a stiffener core material has been designed and developed for aircraft primary structural applications. This stiffener concept is fabricated from textile composite material forms with a resin transfer molding process. This foam-filled hat-stiffener concept is structurally more efficient than most other prismatically stiffened panel configurations in a load range that is typical for both fuselage and wing structures. The panel design is based on woven/stitched and braided graphite-fiber textile preforms, an epoxy resin system, and Rohacell foam core. The structural response of this panel design was evaluated for its buckling and postbuckling behavior with and without low-speed impact damage. The results from single-stiffener and multi-stiffener specimen tests suggest that this structural concept responds to loading as anticipated and has excellent damage tolerance characteristics compared to a similar panel design made from preimpregnated graphite-epoxy tape material.

Introduction

Application of composite materials to aircraft primary structures can have a significant impact on aircraft performance and structural cost. Such applications are expected to result in a 30 to 40 percent weight savings and a 10 to 30 percent cost reduction compared to conventional metallic structures. Realization of these goals requires integration of innovative structural concepts, high-performance composite materials and low-cost manufacturing processes.

A foam-filled, hat-stiffened panel concept that exhibits superior performance compared to more commonly used stiffener concepts was presented in Reference 1. This concept utilizes Rohacell WF71 foam to locate and stabilize the stiffener webs and cap. This approach resulted in a 4 to 8 percent improvement in structural efficiency for prismatic panels compared to a non-foam-filled hat-stiffened panel with a predominantly 0° material cap design for uniaxial compressive loading conditions ranging from 3,000 to 20,000 lb/in. The foam material permits the stiffness of the panel to be tailored by varying the thickness of the 0° material in the stiffener cap during layup. This concept has the advantage that it can be extended to general grid-stiffened structural configurations to provide higher structural efficiencies. As a demonstration of this concept, a prismatic flat panel with foam-filled hat stiffeners made of preimpregnated graphite-epoxy tape material has been designed and evaluated experimentally for a uniaxial compression loading condition similar to that for a transport aircraft fuselage application (Ref. 2). The panel behavior has been evaluated in Reference 2 both with and without low-speed impact damage.

One of the findings reported in Reference 2 is that the residual strength of the foam-filled hat-stiffened panel with low-speed impact damage is about 30 to 40 percent lower than the undamaged panel depending on whether the low-speed impact is at a skin location opposite to the stiffener cap or at the skin and stiffener flange location. Although this level of strength degradation corresponds approximately to the design limit load condition (2/3 times the undamaged panel failure load) for aircraft structures with visible impact damage, it may be possible to improve the residual strength of the panels by using textile materials made with through-the-thickness reinforcement. The prismatic stiffener panel investigated in the present paper utilizes integral weaving, braiding, and stitching technologies to develop a four-hat-stiffener dry-graphite preform for the panel with four longitudinal pockets to accommodate premachined Rohacell foam

* Senior Aerospace Engineer, Structural Mechanics Branch, Structures Division.
Associate Fellow, AIAA.
** Senior Materials Engineer, Mechanics of Materials Branch, Materials Division.

core material. This combination of an efficient foam-filled hat-stiffened structural concept with a more damage-tolerant material form using automated manufacturing processes has the synergy to provide a leading structural concept for aircraft fuselage applications.

The present paper describes an optimum design for a panel with a foam-filled hat-stiffener cross-section that utilizes textile manufacturing technologies in combination with a resin film infusion processing method. This panel is evaluated in uni-axial compression with and without impact damage. Experimental results for both single-stiffener and multi-stiffener panel specimens with and without low-speed impact damage are presented and discussed. Finite element analysis results are presented that predict the buckling and postbuckling response of the test specimens. Analytical results for both the element and the panel specimens are compared with experimental results.

Foam-Filled Hat-Stiffener Panel Design and Development

For the panel design concept used in the present paper, 0° material is placed in the cap of the hat stiffener to increase the bending stiffness of the panel. A design study was performed to select a 30-in.-long by 24-in.-wide panel design with four hat stiffeners that could be made from textile composite materials. The panel design is similar to the panel in Reference 2. The panel was designed to support an axial load of 3000 lb/in. without buckling. A constrained minimum-weight optimization study was performed using the Panel Analysis and Sizing COde (PASCO) described in Reference 3. The material architectures selected for the design were uniweave, braided, and stitched fabric material forms of graphite material with different filament counts and, hence, of different thicknesses. Hercules, Inc. AS4 graphite fibers and Hercules, Inc. 3501-6 epoxy resin were used in this study. Typical mechanical properties used for the fabric, uniweave, braided, and Rohacell foam materials are listed in Table 1. The hat-stiffener dimensions and all laminate thicknesses were variables in the design optimization process. The resulting geometry, material architectures and ply orientations in the cap, web and skin regions of the panel are illustrated in Figure 1.

The sequence of operations for panel fabrication involved several steps. First, a braided sleeve with a ±45° material orientation was wrapped over the premachined Rohacell foam core. Then, a layer of 0° uniweave material was attached to the top of the core with a tackifier before placing the 90° uniweave material onto the core. A second layer of 0° uniweave material was then added to the cap which was then covered with another layer of ±45° fabric material. Additional layers of fabric and uniweave material were added to make up the skin under the hat stiffener and the skin between the hat stiffeners. The skin plies and the skin-stiffener flange plies were stitched together to assemble the panel preform as illustrated in Figure 2. Fabrication of the panel was completed by using the resin film infusion (RFI) process. A solid film of 3501-6 epoxy was cast and placed on a base plate. The assembled preform was located on this epoxy layer, vacuum bagged and cured in an autoclave using the resin-infiltration/cure-cycle developed in Reference 4. The modeling effort described in Reference 4 involved characterizing the permeability of each of the preform regions, quantifying the viscosity and cure kinetics of the resin, and performing finite-element-based flow simulations with various boundary conditions. A photograph of the finished panel is shown in Figure 3. Due to the tooling concept used for fabricating these panels, the stiffener caps had kinked fibers at their centerline running along the length of each of the four stiffeners.

Test Specimens and Experimental Setup

A total of six 30-in.-long by 24-in.-wide test panels were fabricated. Two of these were cut up to produce four 30-in.-long single-stiffener specimens for performing stiffener crippling tests with and without impact damage. Single-stiffener specimens with a shorter length were fabricated using a third panel to generate additional damage tolerance information for this structural concept. Shorter single-stiffener specimens (6.75-in. long) were designed such that the skin buckles into three half-waves to represent the response of the 30-in.-long crippling specimens which buckle into seven half-waves. The ends of both the large panel and the single-stiffener specimens were potted, and machined flat and parallel to introduce the applied load. Both types of single-stiffener specimens were tested as wide columns. The sides of the large panels were simply supported using knife edges to prevent the unsupported skin from buckling and prematurely initiating panel failure. The location of the strain and displacement measuring instrumentation was based on finite element analysis results for both the single-stiffener and panel specimens. The strain gage instrumentation was located at the mid length of the single-stiffener specimen on the stiffener cap, skin, and skin-stiffener flange locations. For the two large panel tests, additional gages were placed at other locations as well. Displacement transducers were used to monitor specimen end shortening and out-of-plane displacements at appropriate pre-determined locations and shadow moiré interferometry was used to obtain a field view of the out-of-plane displacement contours. One four-stiffener panel was tested to generate the undamaged panel results and a second panel was used to perform a damage tolerance test. The impact-

damage conditions for the later test were based on the single-stiffener specimen test results.

Results and Discussion

In the experimental program, two types of specimens were tested which are shown in Figure 4. The first type of specimen consists of single-stiffener specimens of two different lengths shown on the right side of the figure. These specimens are tested in uniaxial compression to determine the critical impact damage conditions for this structural concept when subjected to airgun and dropped-weight impacts. The second type of specimens are multi-stiffener specimens which were tested in compression with and without combinations of airgun and dropped-weight impact damage conditions selected from the single-stiffener specimen test results. The objective of these tests was to gain an understanding of the damage tolerance characteristics of the foam-filled hat-stiffener textile composite panel concept.

Finite element analysis of the single- and multi-stiffener specimens was performed to correlate the undamaged specimen behavior with test results. The DIAL finite element code (Ref. 5) was used to perform buckling and nonlinear static analyses. The finite element models were generated using shear deformable plate elements. Linear static and bifurcation buckling analyses were performed prior to testing the specimens to help make instrumentation and loading decisions. The geometrically nonlinear analyses were performed after the test to correlate the displacement and strain results. Nonlinear analysis results are obtained by using the Newton-Raphson method. The experimental and analytical results are compared wherever appropriate.

Impact Energy Levels for Barely Visible Damage Initiation

Two of the single-stiffener specimens were dedicated to perform impact studies to determine the threshold energy levels for damage initiation at different structural locations. The selected locations are at the stiffener cap, the skin opposite to the stiffener cap, and the skin-stiffener flange interface. The latter two locations were determined to be the most critical for panels made of preimpregnated tape material. Dropped-weight (2.5 lb mass impactor with a 0.5-in.-diameter hemispherical tip) and airgun-propelled 0.5-in.-diameter aluminum-ball impactor tests were performed at increasing energy levels to determine the threshold levels. The damage initiation threshold energy levels for the skin and skin-stiffener flange interface subjected to airgun impacts from the skin side of the panel are 1.60 ft-lb (125 ft/sec) and 3.06 ft-lb (175 ft/sec), respectively. The stiffener cap of the specimens was impacted with a dropped-weight impactor to simulate impact due to dropped tools. Since the stiffener cap did not have a flat surface, it was not possible to get a normal impact on this surface. To compare the damage tolerance results for the textile composite panel with those for the tape-laid composite panel in Referecne 2, a dropped-weight impact-energy level of 20 ft-lb was used for impacts at the stiffener cap and the skin-stiffener interface locations for the textile composite panel.

Single-stiffener Specimens

As the undamaged 30-in.-long specimen was loaded quasi-statically, the skin buckled at approximately 21,000 lb, and further loading of the specimen resulted in failure at a load of approximately 25,600 lb. This buckling load corresponds to 3,300 lb/in. which is greater than the design load of 3000 lb/in. The maximum strain at failure was approximately 6,200 μ in./in. The out-of-plane displacement contours for the specimen with a compressive load of 21,100 lb are presented in Figure 5 and compared with the corresponding analytical results. From the moiré interferometry results and strain gage data it appears that the element specimen skin buckled into seven half-waves at a load of approximately 21,000 lb. The analysis predicts this first buckling mode to occur at 19,900 lb with six half-waves. This discrepancy in buckling results may be due to the non-realization of global bending that was exhibited by the specimen in the test. At the instant of failure, the specimen exhibited the same out-of-plane displacement pattern and the skin had seven half-waves along its length in addition to global bending. The nonuniformity in loading is the potential cause for the unsymmetric out-of-plane deflected shape for this specimen. Failure of the specimen occurred across the width at approximately 1/3 of the length of the specimen which corresponds to the nodal line between the second and third half-waves of the deformed skin which is a location of high interlaminar stresses. The failure is characterized by a clean break of the specimen instead of the ply splitting in the 45° plies and skin-stiffener separation associated with the preimpregnated tape material specimen failure and is shown in Figure 6.

The second 30-in.-long single-stiffener specimen was compression tested after subjecting the stiffener cap to dropped-weight impact. This test was intended to study the response of the single-stiffener specimen in the presence of impact damage due to dropped tools in a structural assembly or maintenance environment. After subjecting the stiffener cap to an impact energy level of 20 ft-lb at mid length, the specimen was loaded in compression. This specimen failed at a load of 11,400 lb. This test was repeated on another 30-in.-long single-stiffener specimen which also failed at 11,300 lb suggesting that when the cap

region with fiber wrinkling is impacted, the damage state is very severe and causes a 50 percent reduction in the specimen strength. The fiber wrinkling is an artifact of the tooling used for manufacturing, and this result is not anticipated in the actual structure which would be manufactured using an improved tooling design. For this reason, this impact condition was not investigated any further.

The third 30-in.-long single-stiffener specimen was tested with a 20 ft-lb dropped-weight impact on the skin side at the skin-stiffener interface. The specimen failure mode was very similar to that of the single-stiffener specimen without damage and occurred away from the impact location. The failure load was 25,200 lb which suggests that the specimen strength did not degrade significantly as a result of this 20 ft-lb impact-energy condition.

Two other 30-in.-long single-stiffener specimens were tested with airgun impact damage to the skin opposite to the stiffener cap. The impact speed for the first specimen was 175 ft/sec, an impact condition which represents a 40 percent higher energy level than the energy level for which barely visible impact damage occurs. For the second specimen, the airgun impact speed was at 350 ft/sec, which represents a near penetration damage condition. The first specimen behaved like the undamaged specimen and buckled at a load of 21,100 lb with seven half-waves and failure occurred at a load of 25, 800 lb. The specimen with the 350-ft/sec impact damage had a buckling mode with five half-waves at approximately 23,200 lb when the specimen failure occurred. This load value corresponds to a 9 percent reduction in strength compared to the undamaged specimen. The failure location for both of these specimens was through the impact location and a typical failure mode for this specimen is shown in Figure 7. The 30-in.-long single-stiffener specimen results suggest that the foam-filled hat-stiffened textile panel has good damage tolerance characteristics, and dropped-weight and airgun impact damage does not significantly reduce the strength compared the foam-filled hat-stiffener panel made from preimpregnated tape material (Ref. 2). The load versus end-shortening results for the 30-in.-long single-stiffener specimens are summarized in Figure 8. The analytical end-shortening results for the undamaged specimen are represented by a solid line in this figure. The comparison between the analytical and experimental results is good. Typical axial strain results for an undamaged 30-in.-long single-stiffener specimen are presented in Figure 9. The onset of nonlinearity in strains occurs at approximately 20,000 lb of applied load and the compressive strain magnitudes at failure are above 5,500 μ in./in.

Out of the five 6.75-in.-long single-stiffener specimens that were available, two were tested without damage to provide reference data and the rest were tested with airgun impact damage either to the skin opposite to the stiffener cap or to the skin-stiffener flange interface along the mid-length of the specimen. The undamaged specimens buckled into three half-waves as shown in Figure 10(a) at approximately 21,200 lb of axial load, and failed at 25,800 lb and 25,300 lb of applied load. The typical failure location for this specimen is shown in Figure 10(b). The next two specimens were impacted at specimen mid-length with an airgun impact-energy level of 12.25 ft-lb (350 ft/sec) on the skin opposite to the stiffener cap and at the skin-stiffener flange interface. These energy levels are 4 to 5 times greater than the corresponding energy levels for damage initiation and result in a considerable amount of damage to the specimens. Both specimens failed before buckling at an applied load of 21,600 lb and the failure was through the damage site. The damage sites and out-of-plane displacement results that reflect damage growth for the specimen with impact at the skin location opposite to the stiffener are shown in Figure 11. The corresponding results for the specimen with impact at the skin-stiffener-flange interface location are shown in Figure 12. The failure load values for these specimens represent a reduction in strength of approximately 15 percent compared to the undamaged specimen failure load. Strength degradations for corresponding impact damage for a foam-filled hat-stiffener panel made of preimpregnated tape material were 31 and 44 percent of the undamaged specimen strength. The last specimen was tested with 20 ft-lb dropped-weight impact at its mid-length on the skin at the skin-stiffene- flange interface location. This specimen failed before buckling at an applied load of 21,700 lb through the damaged site. There is only a 15 percent strength degradation for this specimen with this level of impact damage.

The results from the 6.75-in.- and 30-in.-long single-stiffener specimens confirm the improved damage-tolerance characteristics of the foam-filled hat-stiffener textile material panels compared to those made from preimpregnated tape material.

Multi-stiffener Panel Specimens

The multi-stiffener panels were simply supported along the 30-in.-long edges with knife edges for the uniaxial compression tests. As the undamaged panel was loaded, it exhibited observable out-of-plane displacements in the form of three lobes across the panel width at approximately 48,000 lb of axial load. The panel buckling load was estimated to be 80,000 lb and the resulting buckling mode shape is presented in Figure 13. Further loading resulted in a slightly better definition of the three-lobed mode shape until failure of the specimen occurred at 99,000 lb. The failed specimen and the analytical out-of-plane displacement contour at the failure load are shown in Figure 14. The three-lobed analytical out-of-plane displacement contours can be seen in this figure. As indicated by the

nonlinear analysis results, the largest out-of-plane displacement at the failure load occurs at points away from the potted edges of the panel in the skin between stiffeners. The nodal lines on the skin between the stiffeners corresponding to this deformation pattern are at distances of 1.0 inch and 4.5 inches from the potted ends of the panel and are regions of high through-the-thickness shear stress gradients. The panel failure appears to have initiated at these nodal lines. This failure mode is considerably different from that of the preimpregnated tape panels described in Reference 2, although the failure initiated at lines of maximum interlaminar shear stress in both cases. Due to the textile material forms used in the present study, the failure surfaces are well defined and clean for the textile panels compared to those of the panels made from preimpregnated tape material.

The second multi-stiffener panel was subjected to airgun impact damage at two locations on the skin opposite to the stiffener cap and dropped-weight impact damage at one skin-stiffener flange interface location as shown in Figure 15. The airgun impact speeds were 350 ft/sec and the dropped-weight impact energy was 20 ft-lb. The damage at all locations was extensive as evidenced from this figure. When loaded, this panel failed at an applied load of 89,700 lb which is approximately 8 percent lower than the undamaged panel failure load. The foam-filled hat-stiffened textile panel exhibits excellent damage tolerance for this visible impact damage condition. The multi-stiffener panel end-shortening results are summarized in Figure 16. The experimental end-shortening results for the undamaged panel are compared with the analytical results in this figure. The panel response is nonlinear for loads greater than 65,000 lb. Good correlation is observed between the experimental and analytical end-shortening results until failure occurs.

Concluding Remarks

Design, analysis, fabrication and experimental studies have been conducted to evaluate a structurally-efficient, foam-filled hat-stiffened textile composite panel concept. This structural concept is amenable to automated textile manufacturing processes that can fabricate a dry fiber preform for the stiffened structure into a net shape prior to processing using a resin-film-infusion process.

Single-stiffener specimen test results suggest that airgun impact damage to the skin at the backside of the stiffener cap location at an impact energy level which is 40 percent greater than that for damage initiation results in up to 15 percent strength degradation for this textile composite structure. The strength degradation for the structure made from preimpregnated material is 31 percent. Similar conclusions can be made for a 20 ft-lb dropped-weight impact condition at the skin-stiffener-flange interface location for the textile composite structure. An increase in the airgun impact energy level to approximately 4 times the energy level for damage initiation at either the skin location opposite to the stiffener or the skin-stiffener flange interface location results in a failure load reduction of 15 percent. The corresponding strength degradation level for the preimpregnated tape specimen is 44 percent. This improvement in performance is attributed to the through-the-thickness connectivity provided by integral weaving and stitching of the stiffener elements with the skin elements. In general, the textile composite structure demonstrated better damage tolerance than the structure made from preimpregnated tape material. The global failure strain was greater than 5,500 μ in./in. for all test specimens with and without impact damage which is comparable to the specimens made from preimpregnated tape specimens. For the undamaged specimens which exhibited significant out-of-plane deformations, failure initiated along nodal lines. For specimens damaged with high impact energy levels, failure initiation was through the damage site. The analytical results for the buckling and postbuckling responses compare well with the experimental results.

References

1. Ambur, D. R., and Rehfield, L. W., "Effect of Stiffness Characteristics on the Response of Composite Grid-Stiffened Structures," Journal of Aircraft, Vol. 30, No. 4, July-August 1993, pp. 541-546.

2. Ambur, D. R., "Design and Evaluation of a Foam-Filled Hat-Stiffened Panel Concept for Aircraft Primary Structural Applications," NASA TM 109175, January 1995.

3. Stroud, W. J., and Anderson, M. S., "PASCO: Structural Panel Analysis and Sizing Code, Capability and Analytical Foundations," NASA TM-80181, November 1981.

4. Hasko, G., Dexter, H. B., Loos, A. C., and Kranbuehl, D. E., "Science-Based RTM for Fabricating Primary Aircraft Structures," 39th International SAMPE Symposium, April 11-14, 1994, pp. 779-785.

5. Anon., "DIAL Finite Element Analysis System - Version L3D2," Lockheed Missiles and Space Company, July 1987.

Table 1. Typical mechanical properties for fabric, uniweave and braided forms of graphite-epoxy and Rohacell foam materials.

Property	Material		
	Fabric/Braide Graphite Epoxy	Uniweave Graphite Epoxy	Rohacell Foam
Longitudinal modulus, E_1 (Msi)	9.40	18.50	0.013
Transverse modulus, E_2 (Msi)	9.20	1.64	0.013
In-plane shear modulus, G_{12} (Msi)	0.83	0.87	0.007
Major Poisson's ratio, ν_{12}	0.05	0.30	0.434

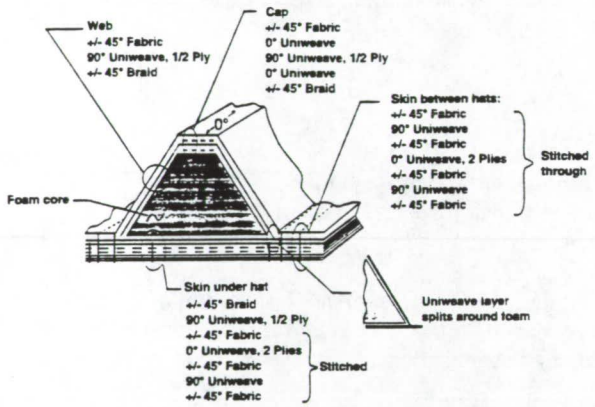

Figure 1. Hat-stiffened textile panel details.

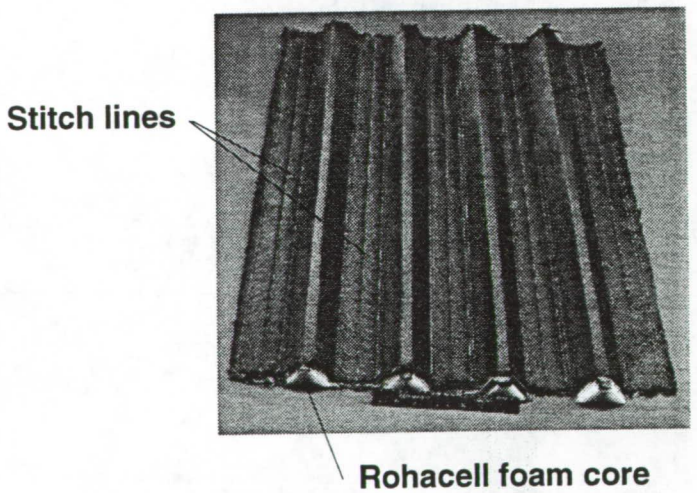

Figure 2. Assembled dry preform before curing.

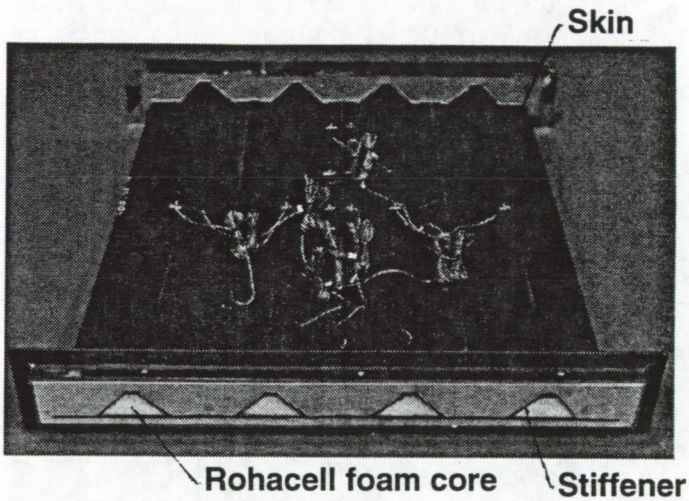

Figure 3. Foam-filled hat-stiffened textile composite panel.

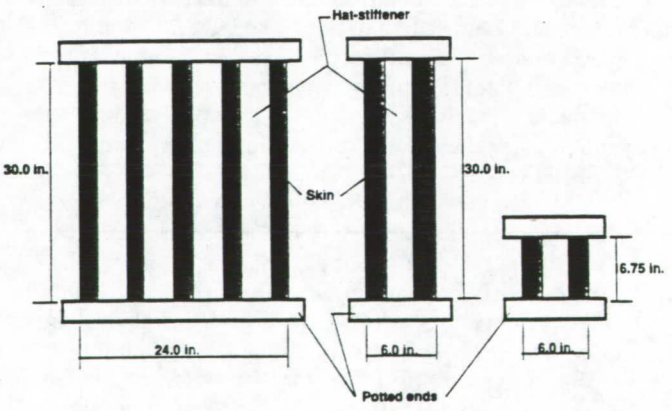

Figure 4. Types of test specimens.

(a) Experimental results

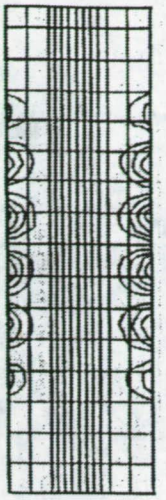

(b) Analysis results

Figure 5. Comparison of analytical and experimental out-of-plane displacement contours for an undamaged 30-in.-long single-stiffener specimen.

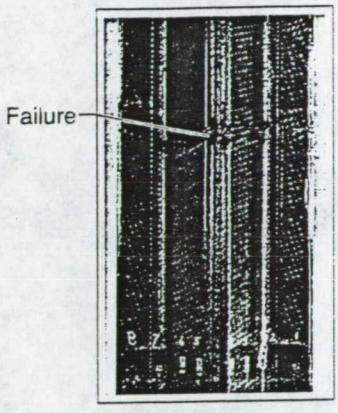

(a) Textile composite

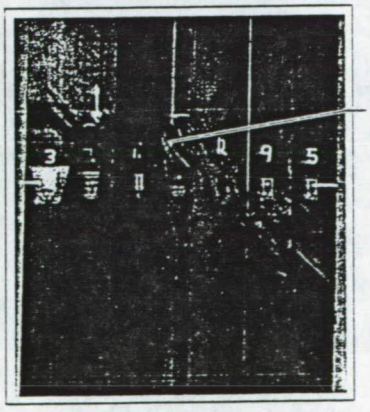

(b) Preimpregnated tape material

Figure 6. Comparison of specimen failure modes made of two different material forms.

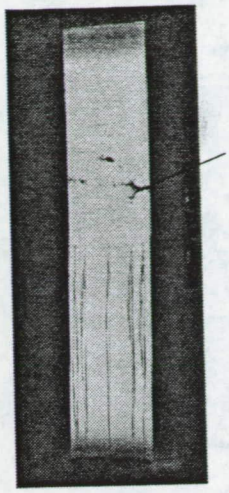

(a) Undamaged panel

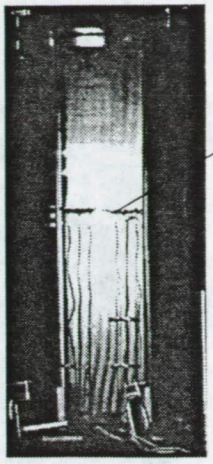

(b) Damaged panel

Figure 7. Comparison of failure modes for undamaged and damaged 30-in.-long single-stiffener speimens.

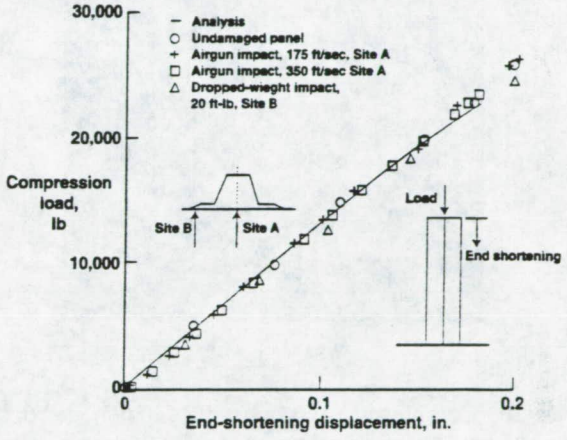

Figure 8. Summary of end-shortening results for 30-in.-long single-stiffener specimens.

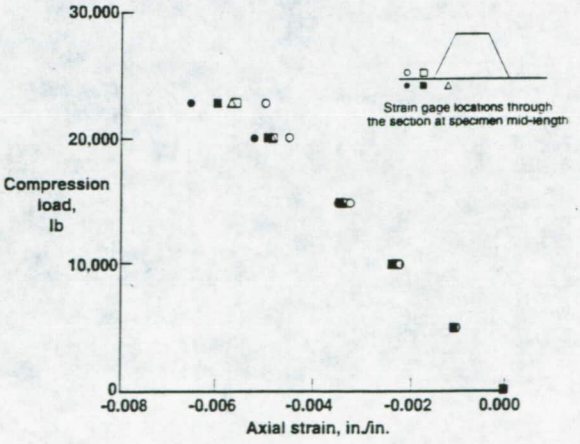

Figure 9. Typical axial strain results for an undamaged 30-in.-long single-stiffener specimen.

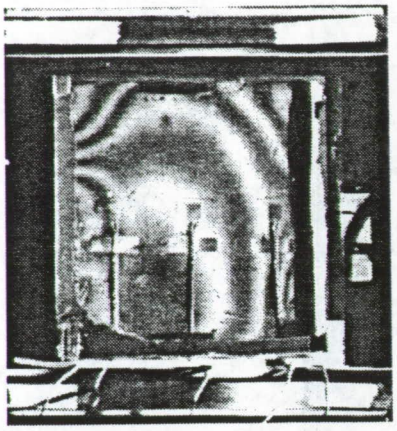

a. Out-of-plane displacement contour

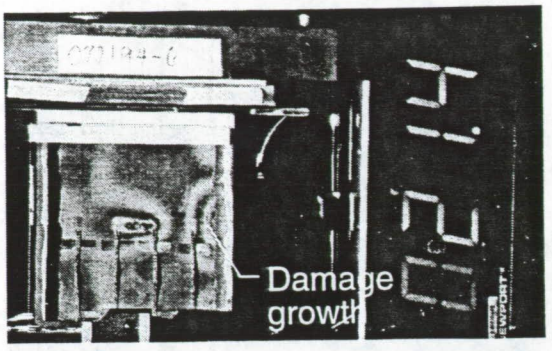

(b) Damage growth

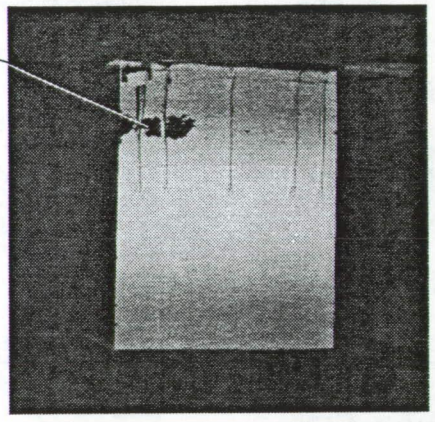

b. Failure location

Figure 10. Compression response of an undamaged 6.75-in.-long single-stiffener specimen.

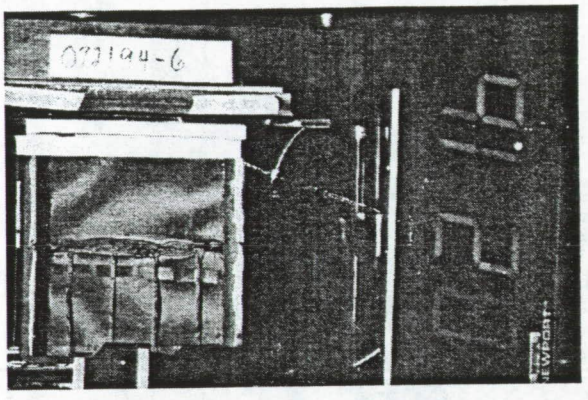

(c) Specimen failure

Figure 11. Compression response of a 6.75-in.-long single-stiffener specimen subjected to 12.25 ft-lb (350 ft/sec) airgun impact at a skin location opposite to the stiffener cap.

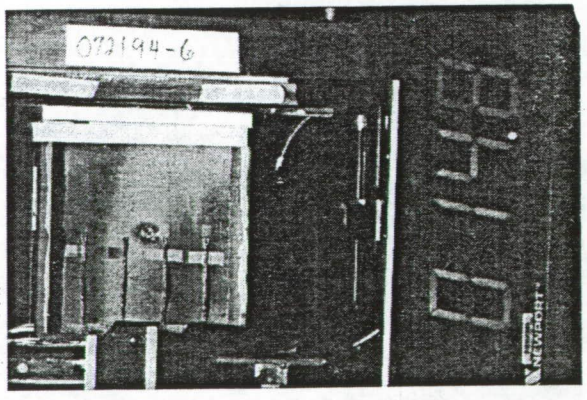

(a) Damage location

Figure 11. Continued.

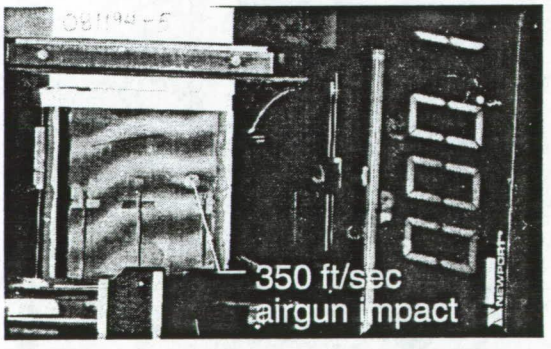

(a) Damage location

Figure 12. Compression response of a 6.75-in.-long single-stiffener specimen subjected to 12.25 ft-lb (350 ft/sec) airgun impact at a skin location opposite to the skin-stiffener flange interface.

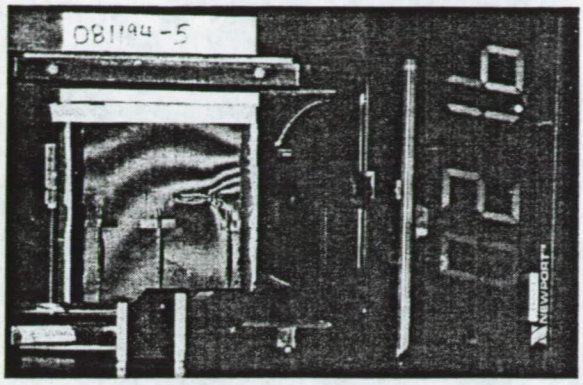

(b) Damage growth and failure

Figure 12. Concluded.

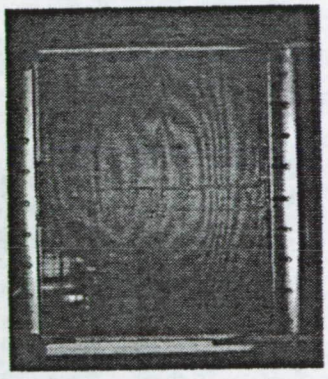

Applied loading 80,000 lb

Figure 13. Undamaged multi-stiffener panel buckling mode shape

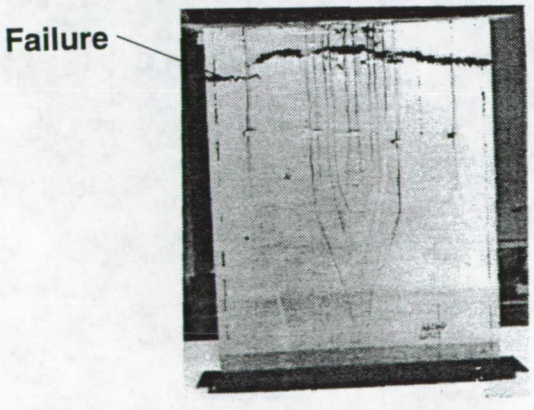

(a) Failed specimen

Figure 14. Continued.

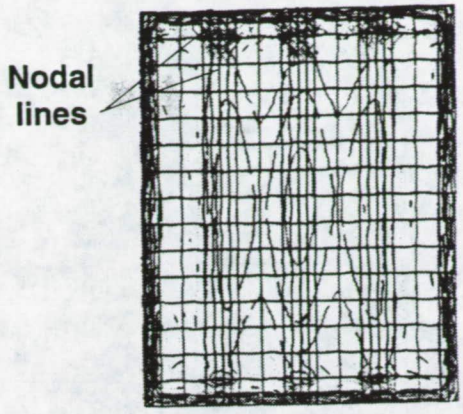

(b) Analytical out-of-plane displacement contour at failure load

Figure 14. Undamaged multi-stiffener panel failure characteristics.

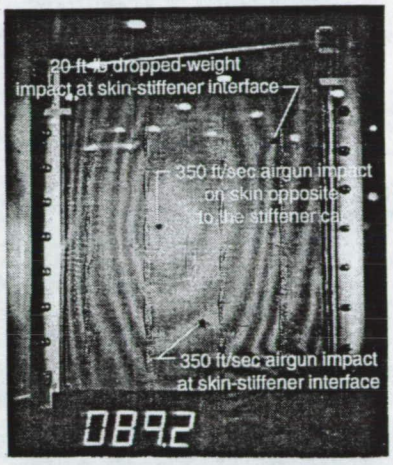

a. Out-of-plane displacement contour at 89,200 lb

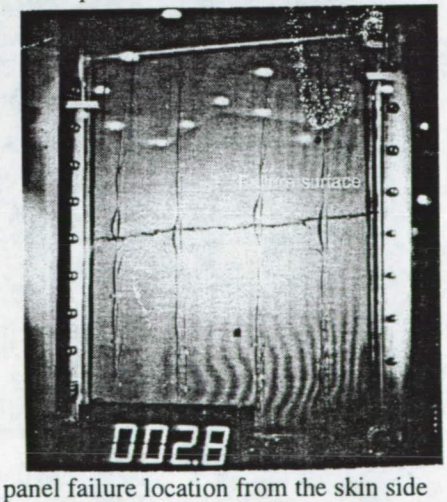

b. View of panel failure location from the skin side

Figure 15. Failure mode of a multi-stiffener panel specimen subjected to airgun and dropped-weight impact damage.

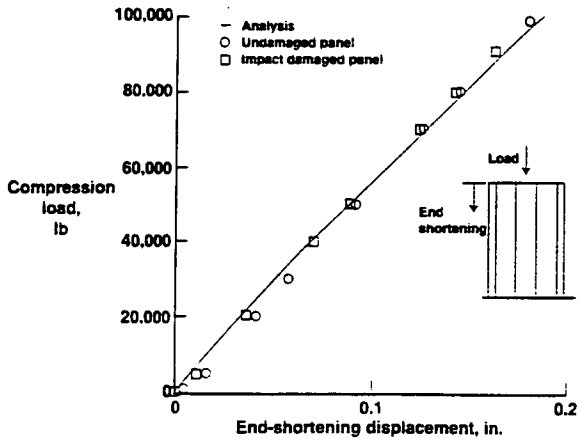

Figure 16. Summary of end-shortening results for the undamaged and damaged multi-stiffener specimens.